Pores in III–V Semiconductors**

By *Helmut Föll*,* *Sergiu Langa*, *Jürgen Carstensen*, *Marc Christophersen*, and *Ion M. Tiginyanu*

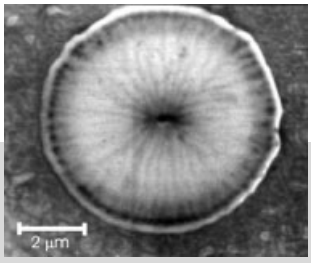

The paper reviews electrochemically etched pores in III–V compound semiconductors (GaP, InP, GaAs) with emphasis on nucleation and formation mechanisms, pore geometries and morphologies, and to several instances of self-organization. Self-organization issues include the formation of single-crystalline two-dimensional hexagonal arrays of pores with lattice constants as small as 100 nm found in InP, synchronized and unsynchronized diameter oscillations coupled to current and voltage oscillations, and pore domain formation. The findings are discussed in relation to pores observed in silicon. Some novel properties of the porous layers obtained in III–V compounds are briefly described.

1. Introduction

In the last decade the discovery of luminescent microporous Si[1,2] triggered considerable interest in porous semiconductors, which in the meantime is fuelled by other kinds of pores and their properties, too. By now, products relying on porous Si are not a dream anymore—they are reality in the ELTRAN process used by Canon to produce "SOI" (Si on insulator) wafers on an industrial scale.[3] More applications are envisioned; for a review see Wehrspohn and Schilling.[4]

Meanwhile, porous semiconductors other than Si are receiving more interest, the most noteworthy being III–V compound materials (and SiC which will not be covered here).[5,6] As will be shown in this review, pore formation in these materials provides for interesting research in its own right, but porous III–V compounds also exhibit new properties[7] with a large potential for applications.

While electrochemical etching (or "anodization") is not the only technique to produce porous materials, it is the most appropriate and versatile one, and this paper will be restricted to electrochemical pore etching. The present knowledge about the formation of pores in GaAs, InP, and GaP will be summarized; some new (mostly optical) properties will be briefly mentioned.

Pores in III–V compounds are not a new discovery, just as pores in Si pre-date 1990. Pores found somewhat fortuitously after the anodization of III–V compounds have been reported as early as 1972,[8,9] when what we would now call "crystallographically oriented pores" were observed. However, much progress has been made during the last five years, and this paper will focus on these more recent developments; for other accounts the reader is advised to consult the literature.[10,11] More noteworthy in recent years are perhaps the many instances of self-organization encountered in III–V pore formation, e.g. self-organized pore single-crystals in InP with periodicity in three dimensions.[12]

2. New Properties and Possible Applications of Porous III–V Compounds

Many III–V compound semiconductors (including the indirect semiconductor GaP) exhibit efficient electroluminescent behavior and thus are widely used in optoelectronic devices. Optical properties are of main interest and while the (electro)optical properties of bulk materials are well known, porous III–V compounds show a number of new and rather interesting properties which will first be enumerated and then briefly discussed.

- A sharp increase in the intensity of the photoluminescence (PL) in porous GaP along with the emergence of blue and ultraviolet luminescence.[13–15]
- A strongly enhanced quantum efficiency of the photoresponse during pore formation in n-GaP electrodes[16,17] and enormous light-scattering in the porous medium.[18–20]
- Strong effects on the intensity of cathodoluminescence (CL): In InP the intensity from porous layers is strongly reduced, while in GaP the intensity is drastically enhanced.[21]

[*] Prof. H. Föll, S. Langa,[+] Dr. J. Carstensen, Dr. M. Christophersen, Prof. I. M. Tiginyanu[+]
Faculty of Engineering, Christian-Albrechts-University
D-24143 Kiel (Germany)
E-mail: hf@tf.uni-kiel.de

[+] S. Langa, Prof. I. M. Tiginyanu, Laboratory of Low Dimensional Semiconductor Structures, Institute of Applied Physics, Technical University of Moldova, 2004 Chisinau, Moldova.

[**] This work was supported by the Deutsche Forschungsgemeinschaft (DFG) under the grants No 436 MOL 113/2/0-1 and FO 258/4-1.

  0935-9648/03/0302-0183 $ 17.50+.50/0

- A more than hundred-fold increase in the optical second harmonic generation (SHG) in porous GaP membranes.[22]
- Evidence for birefringence in porous InP at wavelengths suitable for optical communication systems ($\lambda = 1.55$ μm).[23]
- Porosity-induced modification of the phonon spectrum in GaP, GaAs, and InP.[24–26]

The observation of ultraviolet luminescence is surprising considering that the bandgap of bulk GaP is only 2.25 eV (corresponding to green light). It was speculated that porosity induces the (local) widening of the bandgap to values of up to 3.5 eV by some kind of quantum confinement. While general pore dimensions were probably in the 50 nm region, parts of the "skeleton", i.e., parts of the pore walls, might include structures with even smaller dimensions leading to quantum effects; but this not yet certain.

Bandgap widening and the resulting blue and ultraviolet luminescence in porous GaP always occur simultaneously with new surface-related vibrational modes;[15] a similar situation has been reported in a study on porous Si.[27] Liu and Duan reported surface-related vibrational modes in InP as well and showed that photoluminescence emission of porous InP is very sensitive to heating and chemical treatment. This was taken as an indication that surface states are involved in this radiative recombination. In addition, they found that photoluminescence energy quanta depends strongly on the excitation levels, which is explained by filling effects of the surface states.[28–30]

Similarly, the much larger surface of porous materials and thus the much larger density of non-radiative recombination centers may efficiently quench the cathodoluminescence as observed in porous InP. However, the situation is radically different in GaP, where the cathodoluminescence intensity from porous layers increases substantially.[21] This is not understood at present, but it could be related to the coverage of the surface with oxide which may lead to a lower density of non-radiative surface defects. In addition it must be kept in mind that GaP is an indirect semiconductor which only has an efficient radioactive recombination channel if localized excitons are present, usually provided by isoelectronic doping with N.[31]

The enhanced quantum efficiency of the photocurrent in GaP during anodization is intriguing with respect to the photoconversion efficiency of optoelectronic devices. It might simply be due to the following two effects: a) more effective absorption of long-wavelength light by scattering in the porous layer, and b) more effective capture of the minority carriers at the interface, due to the fact that the dimensions of the porous structure are comparable to the hole diffusion length, i.e., the geometry allows all photo-generated holes to reach the semiconductor/electrolyte interface notwithstanding their small diffusion length.

It is evident that porosity will decrease the refractive index of the material and, under definite conditions, will show different refractive indexes for different polarization of the light, i.e., porosity-induced birefringence. Kikuno et al. reported the refractive indexes parallel ($n_o = 2.82$) and perpendicular ($n_e = 2.66$) to the axes of pores in InP[23] which amounts to a reduction of 11 % or 16 %, respectively, relative to the refractive index of bulk InP ($n = 3.17$). This anisotropy is of particular importance for nonlinear optical applications. While it is well known that III–V compounds exhibit large nonlinear optical coefficients, this feature could not yet be used due to high dispersion and lack of birefringence which is necessary for phase-matching.

Introducing anisotropy into GaP by making it porous allows to generate very strong nonlinear effects, in particular a more than hundred-fold increase of SHG.[22] This enhanced optical SHG is confined to porous membranes of GaP containing pores with triangular cross section, and is attributed to giant third order electric field fluctuations which occur at sharp edges of the pores.[32] Together with birefringence allowing for phase-matching, porous GaP might be used as superior material for frequency upconvertors.

As in the case of Si, for which many potential applications will no longer exploit the semiconducting or optical properties of the material, porous III–V compounds might have uses beyond optoelectronic or nonlinear optics too, since, as will be shown, there are pore structures which are possible and that cannot be produced in Si.

3. Dissolution Mechanisms and Current–Voltage Characteristics

3.1. Materials and Doping

III–V compounds, with the exception of nitrides, crystallize in the cubic zinc blende lattice structure. The crystal consists

Helmut Föll received his PhD degree in Physics in 1976 from the University of Stuttgart in conjunction with the Max-Planck-Institute for Metal Research, also in Stuttgart. After post-doctoral work at the Department of Materials Science and Engineering at Cornell University and a position as guest scientist at the T.J. Watson Research Center of IBM in Yorktown Heights, he joined Siemens in 1980, working in the newly founded Solar Energy Department of Central Research in Munich. After various senior positions in microelectronics development, in 1991 he accepted an offer of the Christian-Albrechts-University of Kiel to become the founding Dean of the newly established Faculty of Engineering, where he also holds the chair for General Materials Science. Since 1998 he is back to research, with particular interest in solar cell technology and the electrochemistry of semiconductors. He is one of the pioneers in the field of porous semiconductors and has co-authored more than 150 papers and 20 patents.

  0935-9648/03/0302-0184 $ 17.50+.50/0

ADVANCED MATERIALS

of two cubic, surface-centered sublattices being shifted relative to each other by the translational vector (¼;¼;¼) . Each sublattice is occupied by one kind of atom from group III or V, respectively. So far the III–V materials most thoroughly investigated with regard to porous structures are GaAs, InP, and GaP.

As in the case of Si, the III–V samples investigated have low index orientations, mostly (100) or (111). The doping level of the substrates subjected to anodization was always between 10^{16}–10^{18} cm^{-3}; more extreme doping concentrations have not yet been tried. With respect to doping, there is a major difference to pores in Si: While in Si pores of all kinds have been found in n-type as well as in p-type samples,[33,34] pores in III–V compounds are so far restricted to n-type material. Attempts (mostly unpublished) of several research groups to produce pores in p-type III–V compounds did not yield the desired results, for a possible, but rather inconclusive exception, see the work of Schmuki et al.[35] On p-type samples electropolishing seems to be prevalent in the experiments performed to date. Therefore, one of the challenges with respect to pores in III–V compounds, is to either produce pores in p-type substrates, or to demonstrate that this is generally impossible.

3.2. Dissolution Chemistry and Electrolytes

Taking into account that electrochemical pore formation is a special case of dissolution (or etching), we will discuss briefly the general etching mechanisms proposed for III–V compounds. Three main dissolution types are distinguished: chemical, electroless, and anodic dissolution.

As suggested by Gerischer and co-workers,[36] chemical etching does not involve free charge carriers; it proceeds independently of an additional potential that might be applied and thus may be present during anodic dissolution, too. It is now generally accepted that during chemical etching a synchronous bond-exchange occurs between undissociated molecules in the solution and the atoms in the solid. As a result, the bonds between the atoms in the solid break and new bonds are formed with reactive molecules in the electrolyte. In order to etch III–V compounds chemically, one typically needs non-oxidizing asymmetric chemical etchants, such as undissociated HCl, HBr, or oxidizing symmetric etchants like Br_2 or H_2O_2, that are capable of breaking the III–V bonds and to subsequently saturate the resulting dangling bonds. The chemical etching rate therefore depends strongly on the concentration of undissociated molecules in the electrolyte.

In contrast, electroless and anodic dissolution rely on the exchange of electrons and/or holes between the semiconductor and the electrolyte and may occur in mixed form. Both processes require at least one hole in order to proceed.

In most cases six holes are required in order to finish the dissolution of a III–V atom pair, although in principle eight holes are needed to remove the two atoms separately, i.e. not as a pair. This can be exemplified by gross reaction equations

$$GaAs + 6\,OH^- + 6\,H^+ = \tfrac{1}{2}\,Ga_2O_3 + \tfrac{1}{2}\,As_2O_3 + 3\,H_2O \quad (1)$$

$$InP + 4\,OH^- + 8\,H^+ = In_2O_3 + In(PO_3)_3 + 2\,H_2 \quad (2)$$

There are two fundamentally different possible means to maintain the necessary hole supply. First, a strongly oxidizing agent in the solution may be able to extract electrons from the valence band, i.e., from a III–V bond, and this is equivalent to injecting a hole. The remaining electron in the bond is now in an excited state (or surface state) and may be removed (relatively easily) by another oxidation event. The reaction chain continues until all bonds are broken and dissolution is complete. This explanation is of course oversimplified and only serves to give a basic idea of an electroless dissolution process.

Second, positively biasing the electrode in an anodic etching experiment induces holes present in the semiconductor to move towards the surface where they are consumed in an electrochemical etching reaction. The spent holes are replaced by current from the external circuit which is required in this case. If all holes are supplied by the current source, a pure anodic dissolution occurs.

The real situation, however, is much more complicated since both processes are usually mixed. The excited electron remaining after the first bond-breaking by an oxidizing agent might, e.g., transit to the conduction band and flow through the external circuit; we then have an electron-injection component in the externally flowing current.

The total charge per III–V atom pair which is transferred into solution (the valency of the process) that flows through the external circuit might therefore be smaller than 6 (or 8) elementary charges and might contain hole and electron components. The difference to 6 (or 8) than is due to an electroless dissolution component, and possibly a pure chemical component, too.

One way to distinguish between hole and electron components is to measure the (reverse) current as a function of the number of photons striking the sample. If an electron is injected for every photogenerated hole in an n-type semiconductor, the resulting photocurrent is doubled relative to the hole-current produced by the photons.

Photocurrent doubling is well known from Si[37,38] and has been observed in GaP by Memming[39] and in GaAs by Minks and coworkers.[40] Since each injected electron could be replaced by an electroless reaction step it is safe to assume that direct dissolution with a valence that in principle could have any value between 2 and 8 does occur in III–V compounds.

So far the processes discussed involve direct dissolution, but there also might be indirect dissolution proceeding via anodic oxide-formation and subsequent chemical dissolution of the oxide. Again holes are needed, but since electron injection is

  0935-9648/03/0302-0185 $ 17.50+.50/0

not possible, the valency in this case should always be 8. While there seem to be very few valency measurements in connection with pore formation, Kaneshiro et al.[41] reported a value of 8 for InP. This, together with the observation of an "oxide peak" in the *I–V* characteristics of GaP (see below) can be taken as evidence that direct and indirect anodic dissolution occurs simultaneously in III–V compounds, with the relative strength of the mechanisms depending on all etching conditions. For more details the reader is referred to the work of Notten et al.[42]

The general situation thus is reminiscent to that of Si (see, e.g., Lehmann[43]). However, considering that III–V dissolution processes are intrinsically much more complicated than Si dissolution, that far less work has been done with respect to Si, and that anodic Si dissolution is still not very well understood, it is no surprise that the dissolution processes occurring during pore etching in III–V compounds are rather poorly understood and that much work will be required before a satisfactory picture will emerge.

3.3. Current–Voltage Characteristics

Electrolytes typically consist of anorganic acids such as HCl, H_2SO_4, or H_3PO_4 diluted with water. While in Si a correlation between pore types and basic electrolyte types (oxygen-containing electrolytes allowing for silicon oxide formation, e.g., aqueous HF, vs nearly oxygen-free electrolytes, e.g., HF + organic solvents, see Propst and Kohl[33]) can be made, no such classification has emerged so far for III–V compounds.

Current (I) voltage (V) characteristics, i.e., *I–V* curves, are the most direct manifestation of junction properties. While *I–V* curves of solid-state devices reflect purely electronic properties of the junctions, *I–V* measurements of semiconductor–electrolyte junctions, while still containing information about the electronic state of the semiconductor, also contain the (chemical) factors that determine the kinetics of anodic dissolution. This makes semiconductor–electrolyte junction characteristics far more difficult to interpret than, e.g., p–n junction characteristics. Nevertheless, in the case of Si, certain recurrent features of the junction characteristics could be tied to characteristic features of pore formation. It is thus of general interest to investigate III–V substrate–electrolyte junction behavior with respect to pore formation.

Under anodic conditions the p- and n-type III–V materials behave quite differently; we have, as in the case of Si, a general diode behavior. The forward-current direction needs positive (anodic) bias in the case of p-type doping, and negative (cathodic) bias in the case of n-type doping. For instance, in the case of p-GaAs substrates in acidic solutions, the current in the anodic direction rises rapidly to very high values, in excess of 100 mA cm^{-2} at 1 V, causing electropolishing of the material, while in the cathodic regime the current remains relatively low.[35] In what follows we restrict ourselves to anodically biased n-type III–Vs.

A word of warning is necessary: the current through cathodically biased III–V compounds does not always produce solely H_2 (as in the case of Si)—in the case of InP, for example, extremely poisonous PH_3 may be generated. If an electrochemical double cell is used, the sample back side is necessarily in the cathodic regime and extreme care is necessary when conducting experiments.

The current-limiting factor seems to be the general lack of holes in n-type semiconductors, combined with the space–charge layer below the semiconductor surface that makes electron injection into the conduction band difficult.

In contrast to anodically biased n-type Si, where, at least in low-doped Si, a very small junction leakage current ($< 1\ \mu A\,cm^{-3}$) can be maintained for voltages as large as 100 V, the reverse current in III–V compounds increases steeply with increasing voltage, and pits are formed on the surface as soon as a critical potential, the so-called pore-formation potential (PFP), is reached. The PFP is also called the breakdown potential; it occurs usually at 2–3 V for moderately doped samples. Schmuki et al. measured the *I–V* curves of samples with intact and diamond-scribe-scratched surfaces. The scratched samples showed a PFP significantly lower than the PFP of the intact sample. These results demonstrated that the PFP depends on the number of defects on the surface of the sample, namely it decreases as the number of defects increases.[44–46] The PFP thus can be viewed as the defect-triggered onset of some kind of junction breakdown in areas of locally large electrical field strengths. A schematic representation of the *I–V* curves with an intact and scratched surface of the GaAs sample is presented in Figure 1a.

In contrast to n-GaAs, Tjerkstra and coworkers[47] reported for n-GaP (in H_2SO_4 aqueous electrolytes) that the current does not increase infinitely after the PFP has been reached, but goes through a maximum at a more positive potential, after which it decreases rapidly to a lower value which shows only a weak potential-dependence. Such peaks are usually due to oxide formation, making current flow difficult. Since the oxide formed has to be dissolved before current can flow again, the peak voltage depends somewhat on the voltage scan-rate and the *I–V* curves show a hysteresis (see Fig. 1b).

Figure 1c shows *I–V* curves obtained during pore etching in InP by a new technique that allows one to take an *I–V* curve within a few milliseconds (without encountering problems with capacities). Pore growth is then not disturbed, in profound contrast to conventional techniques, and the example shown demonstrates that current flow is restricted to the pore tips: While the curves shift on the voltage scale with time (indicating increasing diffusion losses with increasing pore depth) they remain unchanged on the current scale, indicating that no current flows through pore walls.

The findings obtained so far show that there is some correlation between salient features of *I–V* characteristics and pore formation, however, it is far too early to draw detailed conclusions.

0935-9648/03/0302-0186 $ 17.50+.50/0

ADVANCED MATERIALS

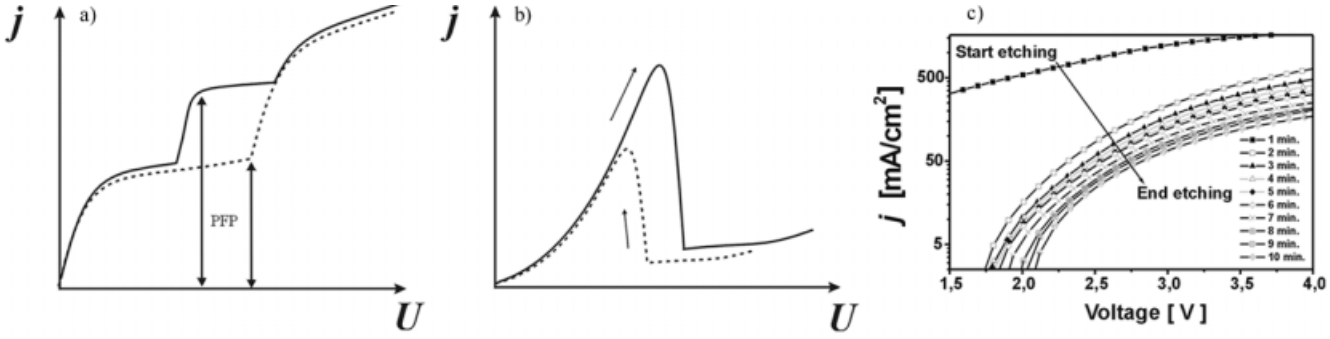

Fig. 1. General behavior of the *I–V* curves in a) GaAs; schematic *I–V* curve; The pore formation potential is smaller for a scratched (solid line) than for intact samples (dashed line); from [45]. b) GaP; schematic *I–V* curve; oxide formation generates the peak and the hysteresis effect in the *I–V* curves; from [47]; c) InP; fast *I–V* curves; the curves shift towards lower currents as the pores grow into the substrate due to diffusion limitations.

4. Overview of Major Pore Properties

4.1. General Remarks

In this chapter we will give a concise overview of the most important features of pore etching in III–V compounds; some of these topics will then be detailed in the following chapters. The most important morphological characteristics together with some other points of interest for pores in III–V compounds are summarized in Table 1 and elucidated below. Silicon has been added as a reference for comparison.

4.2. Pore Geometry and Morphology

With the term "pore geometry" we refer to dimensions only. In order to avoid confusion we will use the standard denominations of micro-, meso-, and macropores from the International Union of Pure and Applied Chemistry (IUPAC)[48] when referring to pores with diameters of < 2 nm, 2–50 nm, and > 50 nm respectively; albeit the usefulness of these designation is somewhat limited for pores in III–V compounds.

The main issue to be studied is the morphology of the porous layers obtained during the anodization of semiconductors. The phrase "morphology of porous structures" in this context refers to individual pore forms (including, e.g., preferred growth directions, branching, diameter oscillations, etc.) and to the properties of porous layers as a whole (e.g., pore crystal formation). The morphology together with the often less important basic geometry define the properties of the resulting structure. Triangular pores in GaP, for example, show strong SHG while round pores with the same geometry do not.[22] Similarly, ordered pore arrays in InP are optically homogeneous, i.e., do not show strong absorption, while random arrays at comparable geometries are not.[49]

Pore morphologies obtained during anodization may differ widely from material to material, and within one material, depending on the precise position in parameter-space chosen for the experiment. Most important in this respect are current density in galvanostatic experiments or voltage in potentiostatic experiments, the sample nature and conductivity, the sample orientation, the nature and temperature of the electrolyte, and the measures taken for the initial pore nucleation.

The pore geometry investigated to date is more or less restricted to macropores; on occasion pores in GaP and InP might be somewhat smaller than the lower limit of 50 nm and must then be classified as mesopores. Note that no micropores

Table 1. Some basic properties of pores in III–V compounds; Si has been added for comparison.

	GaAs	InP	GaP	Si
Doping [cm^{-3}]	n-type 10^{16}–10^{18}	n-type 10^{16}–10^{18}	n-type 10^{16}–10^{18}	p- and n-type 10^{14}–10^{19}
Hole supply	Breakdown	Breakdown	Breakdown	p-doping Illumin. [b] Breakdown
Geometry	Macro	Macro	Macro Meso	Macro Meso Micro
Typical diameter [μm]	0.5–2	0.05–1	0.05–5	0.0011–10
Growth direction	⟨111B⟩	⟨111B⟩ "Current line"	⟨111B⟩ "Current line" Random	⟨100⟩; ⟨113⟩ Random
Growth rates [μm min^{-1}]	1–5	Cryst. pores: 1 Current line: 10–15	Cryst. pores: 1 Current line: 5	Macro: 1 Micro: 1–5
Nucleation	Very difficult	Easy	Difficult	Easy
Self-organization [a]	Diam. osc. IP	Diam. osc. synch. Diam. osc. IP Pore crystal	Diam. osc. synch.	Diam. osc. synch. Diam. osc. IP
Specialties	Domains	"Pillars"	Domains ("Catacombs")	Domains ("Fractal pores")

[a] Diam. osc. synch.: self-induced to synchronized diameter oscillations of all pores; Diam. osc. IP: or diameter oscillations of individual pores. [b] Front- or back-side illumination.

  0935-9648/03/0302-0187 $ 17.50+.50/0

have been observed so far, although, as pointed out above, quantum-confinement effects might exist. This is a bit puzzling because the quantum-wire effect held responsible for micropore formation in Si should be operative in III–V compounds, too. Typical pore diameters and distances between pores are mostly influenced by the doping and seem to reflect the width of the space–charge region.

4.3. Hole Supply

One of the crucial issues in pore formation in semiconductors is the mechanism responsible for the supply of holes to the interface. At least one hole is needed to trigger anodic dissolution, and the abundance or scarcity of holes also determines what kind of dissolution takes place.

Holes can be supplied aplenty by using p-doped specimens; this is however a void option since no pores so far were found in p-doped III–V semiconductors, in contrast to Si. Illuminating n-type specimens also works well in Si and two options are possible: front-side illumination (FSI) and back-side illumination (BSI).

BSI is mentioned because it is the method of choice for the production of high-quality macropores in Si.[50] It is, however, completely useless in all III–V compounds, because the diffusion length of the minority carriers is always far too small to allow the generation of any holes at the back side to reach the reactive interface at the front side.

This leaves FSI (which also allows to generate macropores in Si).[51,52] However, again in contrast to Si, uniform illumination leads to uniform hole generation which usually results in a uniform dissolution of the semiconductor: electropolishing instead of pore etching is obtained. Therefore, FSI is at best useful during the nucleation process of pores.[53]

This only leaves some kind of junction breakdown. Avalanche breakdown of the space–charge layer may produce holes, while at the same time, electrons might be injected, assisted by tunneling or other means, as soon as the electrical field strength reaches some critical value. Electron tunneling through the (top of the) space–charge region, however, is very unlikely for doping levels less than 10^{18} cm^{-3}.[54]

Usually, an avalanche mechanism is assumed to start at surface defects, as e.g., dislocations or scratches. Electron–hole pairs are generated and etching around the defect will occur. The localized etching process induces a pit which will have an increased electrical field strength at its tip—an avalanche process thus is not only self-supporting, but by necessity produces pores with defined dimensions. This general scheme also works in Si, producing (almost) exclusively mesopores; it was investigated in some detail by Lehmann and co-workers.[55]

However, the geometry and morphology of pores in III–V semiconductors are distinctly different from their counterparts in Si. Avalanche breakdown alone cannot account for most pore properties; it may be seen as a necessary but by no means sufficient condition for the understanding of pore formation in III–V compounds. It is important to realize in this context that it is extremely unlikely, if not an oxymoron, to expect a steady-state avalanche situation. It is far more likely that an avalanche breakdown, supplying inexhaustible amounts of holes, induces some rapid dissolution until oxide formation quenches the current flow, and a new avalanche starts somewhere and sometime else. We thus have a general current on–current off situation, and this is the premise of the so-called current-burst model invoked to explain pore formation[56] and current–voltage oscillations[57,58] in Si.

4.4. Growth Directions and Growth Rates

The various aspects of anisotropy in pore growth will be discussed in detail in the next chapter; here only the most prominent features will be mentioned. The growth direction of most pores generally falls into one of two distinctly different groups.

Pores are crystallographically oriented (abbreviated here to "cryst. pores"). So far, the only growth direction reflecting the crystal structure is ⟨111⟩B; the "B" refers to the second element in the compound, e.g., As in GaAs, and P in InP and GaP;[8,59–61] the ⟨111⟩B direction thus points from As to Ga. While it was not always recognized that only ⟨111⟩B is a possible growth direction, experiments show that pore etching on {111}A or {111}B surfaces produces distinctly different results.[8] Note that in Si two cryst. pore directions are found (⟨100⟩ and ⟨113⟩), and that it is too early to definitely rule out this possibility for III–V compounds. While in Si pores never grow in the ⟨111⟩ direction because this direction has the highest density of bonds (and is most easily passivated by H_2),[62] the different chemical reactivities of the atoms constituting the crystal take prevalence in III–V semiconductors and define the essential anisotropic behavior of pore formation.

The pore follows the flow of the current, it is then always perpendicular to the equipotential surfaces in the sample. These "current-line-oriented pores", (or "current pores", for short) thus are mostly perpendicular to the surface, except at edges of the sample where they may curve around, or in branches thrown of by a primary pore. Note that no current pores have been reported up to now in Si. Current pores generally occur at large current densities; they often develop out of cryst. pores. Periodic switching of the current density allows multilayer pore structures to form consisting of alternating layers of cryst. pores and current pores);[9,47] this issue will be discussed in more detail later.

Growth rates for pores can be quite different. While cryst. pores grow, as a rule of thumb, at about 1 $\mu m\,min^{-1}$ (as holds for most pores in Si), current pores can assume growth rates in excess of 10 $\mu m\,min^{-1}$. A 600 μm–thick InP wafer, for example, can be completely penetrated in less than 60 min, compared to about 15 h for Si macropores.

4.5. Nucleation

A particular difficulty in pore-etching experiments with III–V compounds is to obtain homogeneous nucleation of

0935-9648/03/0302-0188 $ 17.50+.50/0

ADVANCED MATERIALS

pores. "Intrinsic" nucleation invariably leads to very inhomogeneous pore structures in GaAs and GaP, in contrast to Si and, to a lesser extent, in InP, where it is easy to achieve homogeneous pore distributions on areas of <1 cm^2.[50,63] The problem is aggravated since III–V compounds always contain dislocations and other defects (in contrast to Si), promoting inhomogeneous nucleation. However, Schmuki and co-workers,[44] and Tiginyanu and co-workers,[64] demonstrated for GaAs and GaP, respectively, that ion implantation into these substrates allows to control the surface defect density and thus to improve the homogeneity of intrinsic nucleation.

Only three attempts to prepare lithographically defined porous structures in III–V materials have been undertaken so far in InP and GaAs.[65–67] These experiments demonstrated, somewhat surprisingly, that this "extrinsic" nucleation seems to be far more difficult than in Si, where pores follow extrinsic nuclei for a wide range of geometries.

Magnetic fields may change the nucleation behavior, as shown for GaAs;[53] other techniques will be elaborated in more detail in what follows.

4.6. Self-Organization

Perhaps the most outstanding feature of pores in III–V compounds are the many instances of self-organization; the most extreme one being the self-organized formation of a three-dimensional pore-single-crystal in InP.[10] A whole chapter will be devoted to this issue. A special feature of self-organization in III–V compounds is the simultaneous occurrence of pore-diameter oscillations and external-voltage oscillations in InP and GaP[68,69] while voltage–current oscillations and pore formation were strictly separate issues in Si.[58] However, similar self-organization issues were now found in Si—after their discovery in the III–V materials triggered a systematic search.[70]

4.7. Specialties

A subgroup of self-organization is the formation of pore domains, i.e., laterally confined regions where pores show evident features of self-organization around a central structure. Distinct domains were observed in GaAs and GaP, while in InP this feature is somewhat hidden. No domain formation has been observed in Si until the recent discovery of the rather exotic "fractal" pores[71] which form clear domains. If etching is continued for a sufficient time, domains start to overlap or fuse, creating a cellular or "catacomb"-like porosity.[64]

Erne and co-workers showed catacomb-like structures in n-GaP surfaces with a (100) orientation after etching in H_2SO_4/H_2O solution.[16] After the initial pitting of the surface in just a few places, further etching proceeds in directions both perpendicular and parallel to the surface until the domains formed in this way meet. Other domain structures have been observed by Föll and co-workers on (100)-oriented n-GaAs samples. The formation mechanism, however, is totally different from that of GaP, as will be shown forthwith.

Of course, this broad picture cannot do justice to the whole range of pore morphologies encountered in anodic etching. Suffice to mention a few of the more interesting features:

Takizawa and co-workers showed that electrochemical etching of a (111)-oriented n-InP surface in a HCl/H_2O solution can lead to a porous layer with a pillar structure characterized by quasi-isolated columns growing perpendicular to the initial surface and an aspect ratio >100.[67] These pillars are probably the remainders of pores that merged, as in a similar case in Si.[72] They also demonstrated that anodization combined with electron-beam lithography can be effective for the fabrication of quantum-wires and box structures. Triangular prism-shaped columns, instead of pores or cellular structures, were also observed by Tiginyanu and co-workers on (111)-oriented n-GaP surfaces electrochemically etched in a solution of HF.[73]

5. Growth Direction and Nucleation

5.1. General Remarks

Pore etching in Si reflects the crystallography of the diamond lattice essentially because of three (related) issues: i) The bond density is different on different crystallographic planes, ii) the passivation kinetics, i.e., the decrease of the density of surface states in the bandgap, due to hydrogen coverage is therefore orientation-dependent,[62] and iii) the (anodic) oxidation kinetic may be orientation-dependent, too.[43] While all these factors may influence the pore growth, an explanation for the preferred ⟨113⟩ orientation in Si has yet to be found.

In III–V compounds, these mechanisms may also be operative, there is, however, a fourth point: iv) III–V compounds have an inherent anisotropy in the chemical and electrochemical behavior because of the difference in chemical reactivity of the constituting elements from groups III and V of the periodic table. The factors determining surface morphology of electrochemically etched III–V compounds have been reviewed by Gomes and Goossens,[74] and Notten and co-workers.[42]

In all oxidizing etching solutions {111}A surfaces show the slowest rate of dissolution,[75] followed by {111}B and {100} surfaces. One possible explanation is the unshared pair of electrons of the B atoms easily available for oxidation. If it is assumed that the rate-determining step of dissolution is the oxidation of the surface atoms, it can be expected that {111}A planes will have the lowest rate of dissolution because of the electrophilic attack of an oxidizing medium. Pore etching in (111)-oriented specimen therefore give completely different results for {111}A or {111}B surfaces and this must always be kept in mind.

It is thus not surprising that pores in III–V compounds reflect the crystallography of the substrates to some extent, and

  0935-9648/03/0302-0189 $ 17.50+.50/0

in ways different from those in Si, and the authors would not be surprised, if new such features will emerge in the future.

5.2. Inhomogeneous Nucleation and Domain Formation

If no special precautions are taken rather inhomogeneous pore structures result in GaAs and GaP for the three major surface orientations (100), (111)A, and (111)B. On {100} surfaces, domain formation and domain overlap are found. Figure 2 shows the essentials of domain formation in (100) GaAs; in Figure 2b an individual domain is seen. The domain formation is caused by multiple branching of two primary pores (nucleated from one nuclei, see below) plus branching of these secondary pores and so on (Figs. 2a,d). The secondary and quaternary pores must grow upwards; their intersection points with the surface form the domain. Note that there is a clear and easily understood alignment of the pore endpoints in one direction (⟨110⟩), and that a cross-section of the domain at some depth below the surface would look quite similar to the structure seen at the surface.

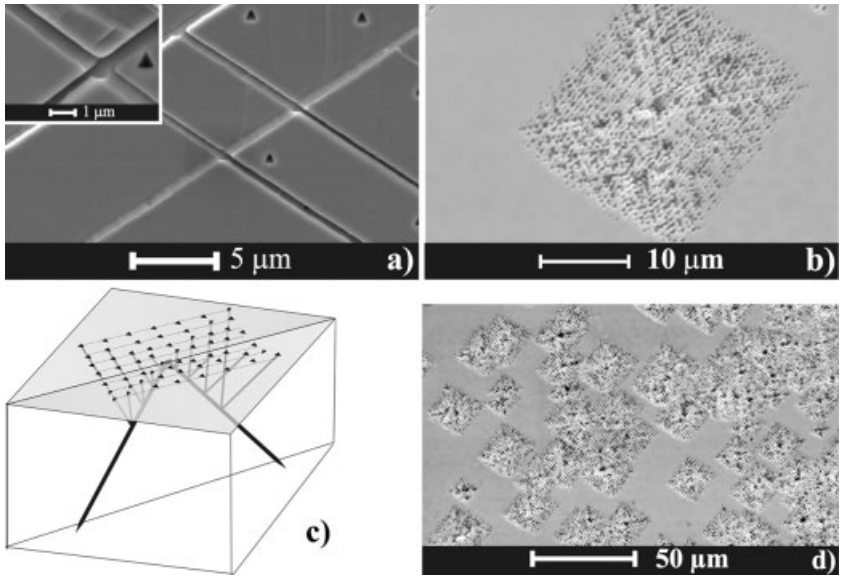

Fig. 2. Pores in a (100)-oriented GaAs sample. a) Cross sectional view of primary pore (not from a domain since the large pore density does not allow one to distinguish individual features). The triangular voids are from secondary pores growing upwards. b) Plane view of a fully developed pore domain. c) Schematic outline of the domain formation. d) Overlapping domains.

The triangular voids seen in Figure 2a are the traces of the secondary pores growing upwards. If they would grow downwards, i.e., away from the sample surface, they would proceed in ⟨111⟩A directions. Indeed, it was assumed earlier that pore growth along all ⟨111⟩ directions is possible, albeit in ⟨111⟩A with a somewhat reduced growth rate.[60,61] However, all observations now are consistent with ⟨111⟩B as the only growth direction for cryst. pores. The authors call ⟨111⟩B directions the ones pointing from B to A planes along the shortest distance between them, i.e., from the most unstable (B = As or P) to most stable (A = Ga or In) planes.[76]

Anodization of n-GaP samples at constant potentials also leads to the formation of domains (sometimes also called catacomb-like pores)[64] as described in detail by Erne et al.[16] The formation mechanism of pore domains in GaP, however, is quite different from that outlined above for GaAs: A few primary pores, nucleated at a defect on the surface, grow into the crystal perpendicular to the surface, generating staggered systems of secondary pores growing away from the central pore like spokes in a wheel (Fig. 3). When individual domains meet, lateral etching stops, leaving visible domain walls, as shown in Figure 3c. The pores expose no evident crystallographic features and thus are current pores; understandable in view of the always very large current density in the few pores.

5.3. Inducing Homogeneous Nucleation

Tiginyanu and co-workers in 1997 first used the damage produced by Kr^+ ion implantation to obtain more homogeneous nucleation in GaP.[64] The same technique has been successfully used by Schmuki and co-workers for GaAs;[44] the authors obtained homogeneous pore growth at a voltage below the PFP of nonimplanted samples. This effect can be used to etch pores within the implanted regions only if the voltage is kept below the pore formation potential of the nonimplanted surface.[44]

Hao and co-workers used an electrochemical pre-treatment for a short time in 50 wt.-% HF in order to form a high density of etch pits in (100) n-GaAs and then anodized in KOH solution to form a high density of pores with uniform distribution. Anodization in KOH without the pre-anodization in HF resulted only in a few large pits on the surface of the sample.[60]

All these pre-treatments are two-step processes, however, necessitating an interruption of the experiment. A one-step process would be advantageous; and one possibility is to use short high-current pulses at the beginning of the anodization

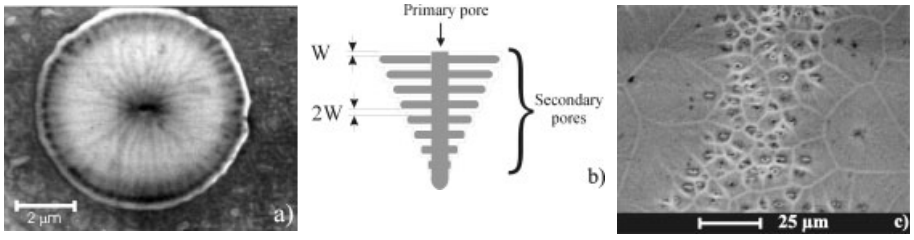

Fig. 3. a) Planar SEM view of a domain (or a "catacomb-like pore") in (100) n-GaP anodized at constant voltages in H_2SO_4 aqueous electrolytes. b) A schematic representation of a domain in cross-section as proposed by Erne et al. [16]. c) Overlapping system of GaP domains. The bright lines denote the domain walls.

0935-9648/03/0302-0190 $ 17.50+.50/0

ADVANCED MATERIALS

process.[77] This seems to work well in GaAs; an example is shown in Figure 4. From the planar view of the sample (Fig. 4a) it is evident that the nucleation is quite uniform and no domains are present; the cross-section (Fig. 4b) shows a

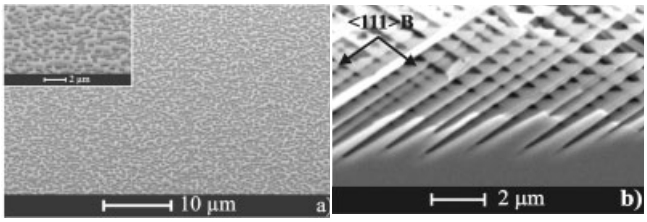

Fig. 4. Uniform nucleation of pores in (100) oriented n-GaAs obtained by initially applying short pulses of high current (H_2SO_4 aqueous electrolytes, $j = 150$ mA cm^{-2} for 3 s followed by $j = 50$ mA cm^{-2} for 5 min). a) Plane view. b) Cross-sectional view.

three-dimensional structure of two kinds of intersecting ⟨111⟩B pores growing only into the substrate. Probably due to the high pore density and thus low current densities in the pores, branching (which is the mechanism for the pore to reduce its current density) has not been observed.

Pores growing relatively homogeneously along ⟨111⟩B directions are not confined to GaAs. The same kind of pores have been obtained in (ion-implanted) GaP and InP—in the latter case no special nucleation treatments are necessary[21,50] (see Fig. 5).

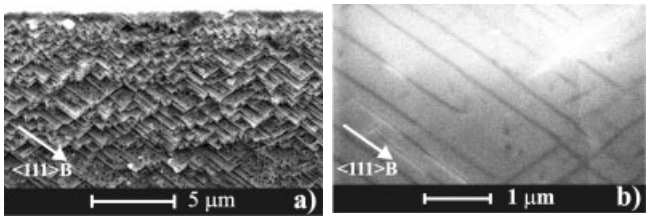

Fig. 5. Crystallographically oriented pores in a) (100) n-InP, anodized in 5 % HCl aqueous electrolyte; b) n-GaP, anodized in 5 % H_2SO_4 aqueous electrolyte. Anodization in both cases has been performed at low current densities (4 and 0.5 mA cm^{-2}, respectively).

5.4. Special Features of Crystallographically Oriented Pores

In elementary semiconductors like Si, there is no difference in A and B planes, nevertheless {111} planes are most stable against dissolution. Therefore, inverted pyramids exposing these planes are obtained with anisotropic etchants, e.g., KOH solutions. Pores in Si mostly grow along ⟨100⟩ directions and the tips of the pores on occasion expose {111} facets. Indeed, pore formation in Si can be viewed as octahedrons bound by all 8 {111} planes,[78] forming out of the initial pyramid (half of an octahedron) which "slide down" in a ⟨100⟩ direction (see also Fig. 6).

The situation is somewhat different in III–V compounds. While in the very beginning of anodic etching a pyramid is formed, as in the case of Si, etching proceeds by elongating the pyramid. An example of a comparison of Si and GaAs has been published by Ross et al.[59] The area of the {111}A bounding planes is increased and the {111}B area decreased, until only {111}A facets are left. The resulting structure has two sharp tips in the form of triangular pyramids (tetrahedrons) which point into the two ⟨111⟩B directions that lead into the bulk of the sample; the formation sequence is shown in Figure 6a.

Anodic dissolution in GaAs follows the same initial sequence (most clearly in GaAs) then continues into the bulk of the sample following the ⟨111⟩B directions defined by the tips. This is certainly due to the fact that the electric field strength at the tip is large,[38] enabling avalanche breakdown. Two pores evolve and can be formally viewed as resulting from tetrahedrons (bound by 4 {111}A planes[79]) that "slide down" the two ⟨111⟩B directions pointing into the sample. In Figure 6b a cross-section scanning electron microscopy (SEM) image taken from a (100)-oriented n-GaAs shows the two pores starting from one elongated pyramid. Such pores then have a triangular cross-section with {112} planes as pore walls,[59,61] confirming the "sliding tetrahedron" picture.

A somewhat unexpected feature of cryst. pores is the ease with which they intersect as shown in detail in Figure 2a. According to some models,[16,38] this should be difficult to impossible because pores should always be separated by walls with characteristic dimensions of twice the thickness of the surface depletion layer. If a pore wall becomes thinner than that, it can no longer support a field perpendicular to the surface which is sufficiently high for anodic hole generation (avalanche mechanism), thus the pore etching should stop.[16] The observation of crossing pores unambiguously demonstrates however, that the unavoidable decrease of the electric field strength at the meeting place is not decisive, or at least that it is still strong enough for hole generation via avalanche breakdown.

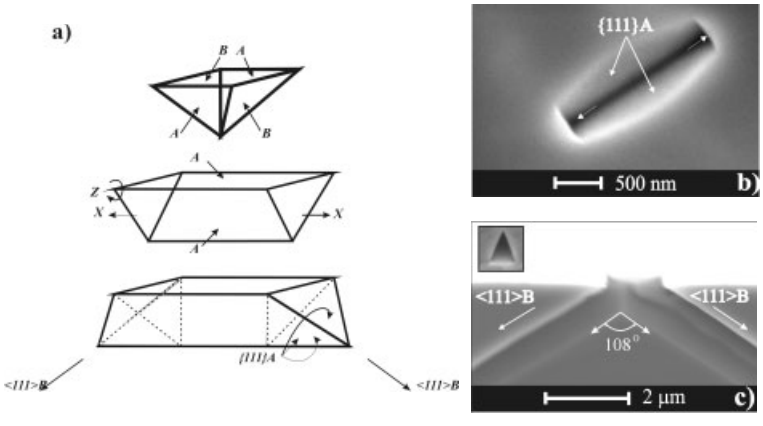

Fig. 6. Pore nucleation in (100)-oriented n-GaAs; a) Schematic illustration of the process converting an initial etch pyramid to an elongated structure with (111)A walls only. b) Plane view of an elongated structure obtained at the beginning of anodic etching in GaAs. c) Cross-sectional view showing the two pores growing in the ⟨111⟩B direction. The inset shows the triangular shape of these pores.

  0935-9648/03/0302-0191 $ 17.50+.50/0

A convincing demonstration of the fact that crystallographically oriented pores in III–V compounds grow along ⟨111⟩B directions is to anodize (111) oriented samples with {111}A or {111}B surfaces. Major differences are expected, found, and shown in Figure 7. For {111}B surfaces, pores grow straight down, while for {111}A surfaces the pores form an angle of 70.5° to the normal of the surface, as is expected.

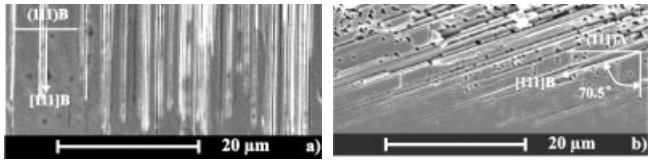

Fig. 7. (111) n-GaAs oriented sample anodized from the a) (111)B surface and b) (111)A surface. The pores grow perpendicular to the surface only if the sample is anodized from the (111)B surface.

5.5. Extrinsic Nucleation Using Lithography

Discounting an early experiment by Carrabba and co-workers,[65] only two experiments have been done so far which used lithographic patterning only to define pore nucleation centers at etching conditions under which stable pore growth already exists. In our opinion Carrabba and co-workers obtained pores in GaAs at etching conditions where normally electropolishing would occur. Only the combination of lithographic mask and front side illumination allowed for local etching and thus for the pore formation.

Takizawa and co-workers[67] used electron-beam lithography on (111)-oriented n-InP samples and obtained triangular pores with diameters in the 100 nm range and aspect ratios >100. Since cryst. pores and current pores would grow perpendicular to the surface, a clear distinction is not possible, but it is very likely that cryst. pores were observed.

Langa and co-workers[77] used conventional lithography to define square and hexagonal arrays of extrinsic nuclei on (100)B n-GaAs with lattice constants between 300 nm and 4 µm; Figure 8 shows some results. From each nucleation point two pores start to grow along ⟨111⟩B directions. However, some parasitic pores start to grow randomly, too. Branching is also observed and both effects together destroy the uniformity of the structure in the depth of the sample as shown in the cross-section (Fig. 8b). This may be taken as an indication that an extrinsically defined structure is only maintained if the extrinsically imposed geometry is closer to the intrinsically favored geometry; a feature distinctly different from the situation in Si.

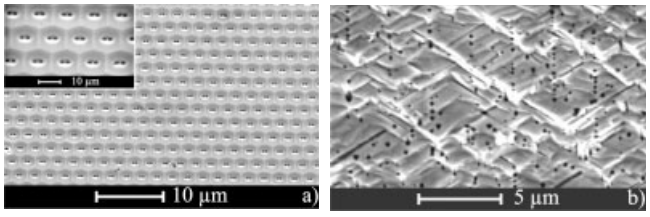

Fig. 8. Lithographicallly defined pores in GaAs. All pores were etched in HCl solution without illumination at $j = 1$ mA cm^{-2}. a) Top view at two magnifications of the pores. c) Cross-sectional view.

5.6. Current Line Pores

The current density in a single pore is probably the most important parameter determining pore geometry and morphology. Under certain, not yet fully explored circumstances it is possible to combine homogeneous nucleation, high initial pore densities (preventing branching and thus the lowering of the current density in pores), and high current densities. This set of parameters induces new features, notably current pores. The most pronounced instances of current pores are found in InP and to a lesser extent in GaP; in GaAs no current pores have been observed so far.

Figure 9 demonstrates current pores by showing an optical microscope cross-sectional image of an InP sample etched at all surfaces simultaneously. Pores grow into the sample from all sides and there is no difference between the (111)A (top) and (111)B (bottom) surface.

Figure 10a shows the formation of current pores in InP out of an initial layer of cryst. pores. This is a general observation;

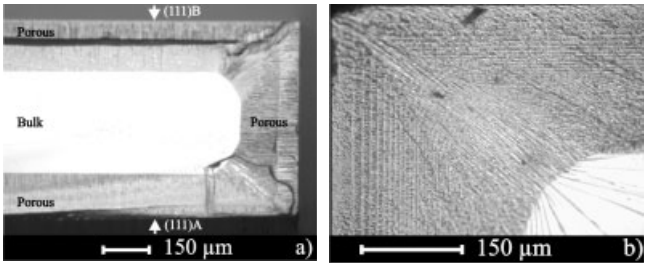

Fig. 9. a) An optical micrograph taken from a (111)-oriented n-InP wafer. The current pores grow perpendicular to the surface from B as well as from A surfaces. b) Detail of pore structure at the corner of the sample. The faint lines result from a short current variation in regular intervals to mark the growth front.

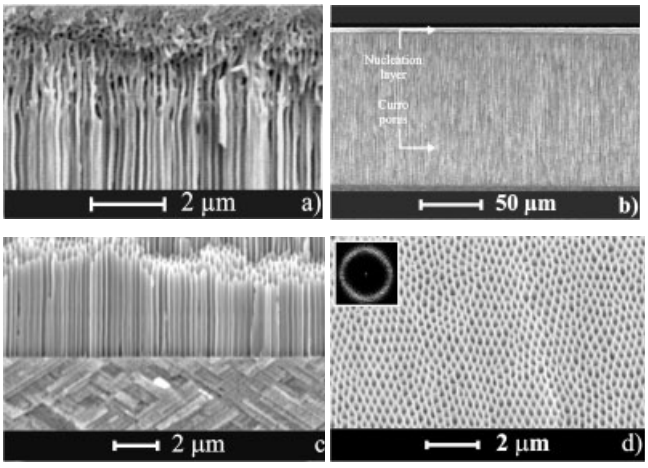

Fig. 10. (100)-oriented n-InP; current line pores vs crystallographically oriented pores. a) The current pores start to grow out of an initial layer of cryst. pores. b) Current pores extending to large depths. c) The switch from current to cryst. pores upon lowering the current density. d) A top-view of current pores showing self-induced ordering; the inset shows the Fourier transform of (a larger area) this picture.

0935-9648/03/0302-0192 $ 17.50+.50/0

ADVANCED MATERIALS

current pores usually need a cryst. pore nucleation layer. Of course, if a (111)B surface is etched, cryst. pores are morphologically indistinguishable from current pores, and the nucleation layer does not manifest itself. After nucleation, current pores grow with unprecedented growth speed of up to 15 $\mu m\,min^{-1}$; the whole sample can be penetrated in about 60 min. Figure 10c shows an example with a very sharp transition from current pores to cryst. pores upon lowering the current density from 70 to 0.5 $mA\,cm^{-2}$. A top-view of the current pores (obtained after removing the nucleation layer) exposes a completely new feature of pore etching in semiconductors: A hexagonally close-packed pore (poly)crystal has formed. Lattice constants between 50–500 nm have been obtained, essentially as a function of doping.

The possibility to change the morphology by controlling the current density allows to produce structures with alternating layers of current and cryst. pores, respectively.[12] Since the porosity of the two types of porous morphologies and thus refractive index is quite different, the multilayer structure shown in Figure 11a is a Bragg-like reflector which can be easily adjusted to desired specifications. Bragg reflectors in Si

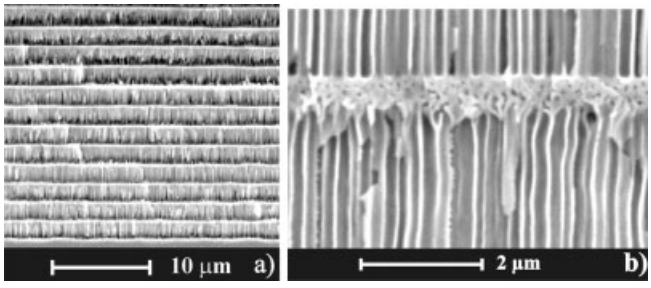

Fig. 11. a) A multilayer structure obtained in n-InP by switching the current periodically from low to high values. b) Detailed representation of the switching from current pores to cryst. pores and back.

made from microporous layers with alternating porosity have attracted a lot of attention;[80,81] the possibility of obtaining Bragg reflectors in optoelectronic materials may thus be even more interesting.

A few comparable experiments have been done in n-GaP. Current line-oriented pores which were essentially perpendicular to the surface, independent of the orientation of the sample, were found, too, but they are distinctly different in appearance from current pores in InP. In particular, current pores in GaP have much larger diameters as compared to current pores in InP obtained at the same doping level (typically 10^{18} cm^{-3}). Current pores in InP have no branches, whereas in GaP some branching seems to occur (see Fig. 12b). Most remarkably, no pore crystals have been found so far.

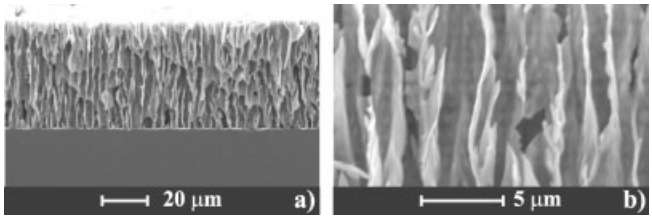

Fig. 12. Current pores in n-GaP ((100), $j = 80$ $mA\,cm^{-2}$, 5 % H_2SO_4, $t = 30$ min. a) Typical structure. b) A detailed magnification of current pores in GaP.

Similarly to the case of InP, Tjerkstra et al.[47] reported that in GaP it is also possible to obtain multilayer structures by changing the porosity and pore size by regulating the potential applied during the anodic etching of n-type material in 0.5 M H_2SO_4. Also the authors did not use the nomenclature used here, it appears that the multilayer structure resulted from switching from cryst. to current pores and back.

6. Self-Organization Phenomena

6.1. General Remarks

Generally speaking, self-organization in porous III–V compounds manifests itself by self-induced oscillations (or periodicities) of pore-system properties in space and/or time. Examples of the first kind are the pore crystals in InP, a manifest periodicity in space. Pore-diameter oscillations, always coupled to current or voltage oscillations in time, are an example of the second kind. While the formation of a pore crystal by definition needs some synchronizing of individual pores, i.e., some kind of interaction that induces every pore to assume the correct position with respect to all the others, diameter oscillations can occur without synchronization, too. Any pore then oscillates its diameter independent of its neighbors, in contrast to synchronized oscillations when all the diameters of all pores increase and decrease in harmony.

It is easy to see that unsynchronized self-organization will not easily be noticed via the external etching parameters, such as etching current and voltage. Current oscillations in individual pores that are not synchronized (or phase-matched), will simply average to fairly constant external current. Only if synchronization occurs in an area comparable to the sample area, macroscopic oscillations in external parameters will be observed.

Self-organization can evolve in space and time, can maintain a stable form, or can show transient phenomena—all of this is observed during pore etching of III–V compounds, and, to a lesser extent, in Si (for a short overview see Föll et al.[10]).

6.2. Pore Crystals in InP

As already shown in Figure 10d, current pores in InP show a tendency to pore crystal formation. In GaP this has not (yet) been observed, and in GaAs no current pores have been obtained so far. The only other known instance of pore (poly)crystal formation is anodically grown Al_2O_3.[82,83] In Figure 10d no long-range order is evident, it is thus a polycrystal even though no clear grain boundaries are seen. A two dimensional (2D) Fourier transform from such pictures results in a relatively sharp ring (see the inset in Fig. 10d).

The degree of crystallinity can be influenced by the etching conditions; at optimized conditions even a single crystalline 2D porous array can be obtained (Fig. 13d).

  0935-9648/03/0302-0193 $ 17.50+.50/0

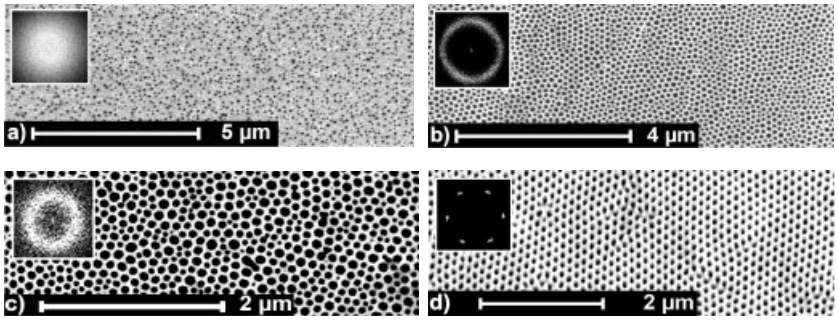

Fig. 13. Pores crystal formation in (100) InP as a function of etching conditions. The insets show Fourier transforms. a) Nucleation layer of cryst. pores; the structure is amorphous. b,c) Pore structure of layers anodized at "low" (b) or "large" (c) voltages showing some degree of order, but no long-range order. d) Pore structure of a layer obtained under optimized current–voltage conditions—a single crystal is obtained. The current pore structure in (111)B-oriented samples behaves similarly, except that the nucleation layer is not as easily visible.

As should be expected for intrinsic., i.e., random nucleation, the arrangement of (cryst.) pores on the surface of the sample is random, and the Fourier transform shows the typical diffuse ring (Fig. 13a). A single pore crystal in the current pore-layer array is obtained for optimized current–voltage conditions (which depend on doping and sample orientation). In particular, the voltage in a potentiostatic experiment is of prime importance—voltages smaller or larger than an optimum value tend to destroy the long-range order (Figs. 13b,c). While the crystal contains many defects like dislocations, its single-crystallinity is clearly demonstrated by the Fourier transform and by long-range order perceptible as soon as the eye follows a major crystal direction.

The observations are consistent with a model that assumes that initial cryst. pores in InP will branch, forming similar domains of cryst. pores as in GaAs (see Figs. 2b–d). Starting from one nucleation point on the surface a monotonically increasing number of cryst. pores (created by branching) is generated in the depth of the sample which are all aligned according to their growth directions. Successive branching can lead to domains of quasi-ordered cryst. pores. The size of the cryst. pore domains increases with the depth of this cryst. pore layer. Since the etched samples are single crystals of InP, all cryst. domains are aligned in the same direction. At high current densities the cryst.-pore growth will switch to current pore growth in a certain depth. The already formed cryst. pores will serve as nucleation sites for current pores transferring the long-range ordering induced by the global alignment and the size of the cryst.-pore domains into current pore domains.

Taking additionally into account the hexagonal short range ordering inside the current domains induced by the repulsive interaction of the current pores via the space–charge regions, all experimentally found degrees of ordering in the InP current pores, in particular their voltage- and the doping-dependence, can be explained.[12]

Since cryst. pores are always necessary as nucleation layer for current pores a diffusion limitation for reaction products or educts is most probably essential to form current pores. This may as well explain the pronounced temperature-dependence of most self-organization phenomena including pore-crystal formation.

6.3. Voltage, Current, and Diameter Oscillations

Voltage or current oscillations are well known from Si electrochemistry (and many other systems), but until recently were confined to the electropolishing regime of Si. They were first explained by Carstensen and co-workers[56] as a manifestation of large-scale synchronization of intrinsically stochastic events; a somewhat modified stochastic approach was later given.[84] The so-called "current-burst model" invoked in the literature[56,58] was subsequently extended to pore formation in Si, but current–voltage oscillations and pore formation in Si were never seen simultaneously until findings from III–V pore etching triggered comparable experiments in Si[70] that revealed voltage oscillations coupled to synchronized diameter oscillations.

In contrast to Si, pronounced voltage oscillations under galvanostatic etching conditions are easy to obtain in InP[66] and GaP,[21] they are always linked to synchronized pore-diameter oscillations; an example is given in Figure 14 and there is a one-to-one correspondence between voltage and diameter peaks.

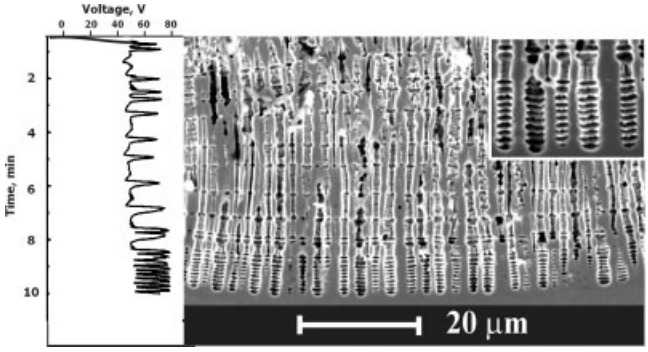

Fig. 14. Synchronized diameter oscillations in InP current pores and simultaneously occurring voltage oscillations. The inset shows an enlargement of the bottoms of the pores.

The situation is different for potentiostatic conditions. While the same mechanisms should be operative and induce synchronized current oscillations, many individually synchronized domains could form, but with random phases between domains. The size of the domains would be given by the correlation length of the synchronizing interaction which must proceed by percolation. The external current then still is constant, if somewhat noisy. This may explain why current oscillations are usually not observed, in addition the constant space–charge region width dictated by the constant voltage may prevent the necessary feedback.

However, if synchronization has been achieved in a galvanostatic experiment, it should be maintained, at least for some time, if the system is switched to a potentiostatic condition that provides (on average) the old current density. In this way

0935-9648/03/0302-0194 $ 17.50+.50/0

ADVANCED MATERIALS

it was indeed possible for the first time to obtain sustained current oscillation during pore growth, as shown in Figure 15.

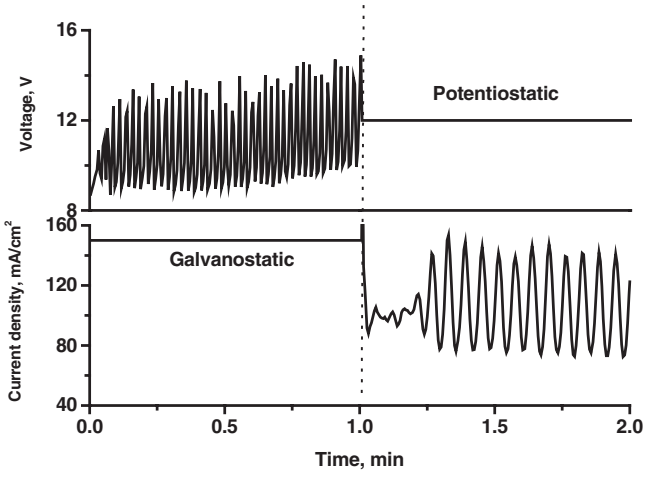

Fig. 15. Switching from galvanostatic to potentiostatic conditions after synchronization was obtained. Self-induced current oscillations were obtained for the first time in this way.

Self-induced diameter oscillations may occur without synchronization, too. In this case no external voltage–current oscillations are observed and the self-organization is only visible in SEM images. The best examples for this are found in GaAs if high current densities are applied for relatively long periods of time in HCl aqueous solutions. This induces multiple pore branching finally resulting in pores showing pronounced diameter oscillations (see Fig. 16). Chains of tetrahedrons are observed which may be seen as an extreme example of the "tetrahedron sliding process" outlined in Section 5.4. An example of such pores is presented in Figure 16a.

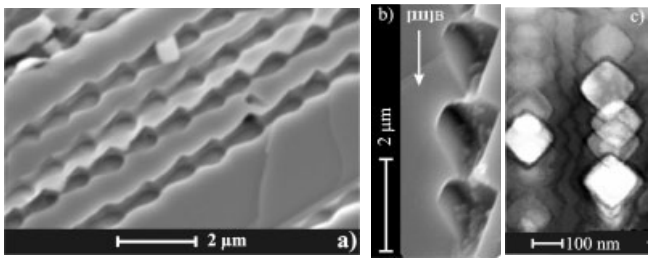

Fig. 16. a) Self-induced unsynchronized diameter oscillations in GaAs. b) Detail, showing the tetrahedra in GaAs and octahedra in Si [78,79]. c) Octahedra in Si (from [78,79]).

"Sliding" obviously proceeds now in a discontinuous way. In Si, similar features can be observed in the context of mesopore formations, then the diameter oscillations express themselves as chains of octahedra; shown for comparison in Figure 16c.

Voltage oscillations under constant external current conditions may be easily understood if we make the (major) assumption that the current at the pore tip generally oscillates (an on/off situation is sufficient) while the diameter may remain nearly constant; the current density then oscillates, too. While this is a far-reaching assumption, it is not only one of the basic premises of the current burst model invoked with for Si electrochemistry,[56,85] but a quite natural occurrence if avalanche breakdown is the sole mechanism for hole generation as outlined in Section 4.2. Space does not allow a detailed discussion, therefore only a brief explanation of the voltage oscillation based on this assumption will be given.

Assuming an intrinsically (and individually) oscillating pore current, each pore may then be described in equivalent circuit terms by an oscillating resistor $R(t)$, with the average value $\langle R \rangle$. The total current is given by switching all resistors in parallel to the current–voltage source. As long as the phases of the oscillating resistors are uncorrelated, i.e., random, the total current will have some constant average value given by $\langle I \rangle = U/\langle R \rangle$ (U = voltage, R = resistance). As soon as the space-charge region around pores starts to touch (always achievable in dense arrays by raising the current), pores will interact. If as a result of this interaction pores start to synchronize their growth, as they evidently do, the phase of the pore currents are now correlated and the current would start to oscillate in a synchronized way. However, the power supply must maintain a constant current, and the only way this can be done is by oscillating the voltage. Since the voltage is the same everywhere on the sample (disallowing lateral currents due to inhomogeneous etching conditions), synchronization by necessity must occur on most of the sample surface.

Essentially this simple model can explain most observations (the big puzzle being the pronounced influence of the temperature).[12] Of course, in a better approximation, one would have to describe a pore by a more complex equivalent circuit containing capacitors C which cause a certain amount of displacement currents $I_{cap} = C\,(\mathrm{d}U/\mathrm{d}t)$. This, however, (and the inherent nonlinearity of the I–V characteristics) will essentially tend to make the voltage swing saw-tooth-like—as is observed.

This consideration, if turned around, gives a clue to the interaction mechanism between neighboring pores. If, by random fluctuation of pore diameters, pores come close enough to experience some kind of influence on their states of dissolution, a feedback mechanism may start that leads to phase-coupling of the pore states and by percolation to the formation of a synchronized domain. The frequency of the voltage oscillations in this model would be determined by the frequency of the current oscillations.

Under galvanostatic conditions, however, domains that only cover parts of the specimen surface will be "killed" by the condition of constant voltage everywhere. Moreover, since percolation does not have to take place at every cycle of the oscillation—especially if the general conditions are just around the percolation point of the system—voltage oscillations might be irregular (as shown in Fig. 14) or may suddenly occur or disappear, as shown in Figure 17 without any discernible external cause.

Figure 17 shows the most impressive case of self-organization obtained during pore etching in III–V compounds, and possibly one of the most extreme cases of self-organization in general: Self-induced strong diameter oscillations occurring simultaneously with self-induced single-pore-crystal forma-

  0935-9648/03/0302-0195 $ 17.50+.50/0

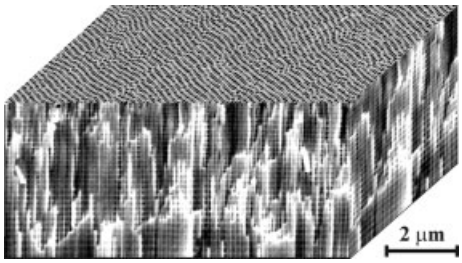

Fig. 17. Single-pore crystal with periodicity in three dimensions (collage of individual SEM micrographs from the same sample) on (100) n-InP, $n = 10^{18}$ cm^{-3}, $j = 100$ mA cm^{-2}, 5 % HCl, $T = 20$ °C.

tion. This is essentially a three-dimensional photonic crystal akin to the one obtained extrinsically in Si,[86] albeit its imperfection does not allow direct applications.

7. Discussion

7.1. General Remarks and Characteristic Length Scales

Many distinctly different models have been proposed to explain pore formation and current–voltage oscillations in Si—the matter is far from being clear.[87] Pore formation in III–V semiconductors provides a wealth of new features; it is thus presumptuous to assume that it can be easily understood. We will therefore refrain from discussing the pro and cons of various models adopted to III–V materials, and only draw attention to the length scale expressed in the pore geometry, and some issues of self-organization.

Pore structures in III–V compounds (and in Si) always have well-defined geometries and thus express a distinct intrinsic length scale of the semiconductor–electrolyte system; compare with Föll et al.[88] The length scale expressed in pore geometry may result from quantum wire effects (nanometer scale), avalanche break-through (10–100 nm scale),[55] space–charge region (10 nm–10 μm), Helmholtz layer thickness (3–5 Å), diffusion instabilities (micrometer to centimeter),[87] or extrinsic scales defined by lithography.

It appears that the intrinsic length scale in III–V semiconductors is much more dominant than in Si. This makes it far more difficult to impose an extrinsic scale that is noticeably different from the intrinsic scale on the system. In other words: Defining pore geometry by lithography will not be successful if the extrinsic scale is not tuned to the intrinsic one.

The major question then is what determines the intrinsic scale? It is too early to give definite answer, but some points can be emphasized:

Avalanche breakdown essentially calls for relatively small pore diameters in order to allow high field strengths at the tips. While quantitative calculations similar to those of Si have not been done so far, it does not appear that the avalanche breakdown scale is of prime importance. To be sure, some parts of the pore tips must be able to produce sufficient field strength, but this does not seem to influence the shape of the pore very much. The best examples for this are cryst. pores in GaAs, which have fairly large diameters far in excess of the typical avalanche scale.

Similarly, no clear expression of scales resulting from quantum confinement, diffusion instability (e.g., Chazalviel and coworkers[87]), or Helmholtz layer dimensions is easily perceived. This does not rule out that these phenomena will not influence pore growth, but gives a motivation to look for other effects as well.

The size of the space–charge region is definitely one of the major length scales found in many (but not all) instances. In particular, it determines rather directly the lattice constant of pore crystals in InP. On the other hand, cryst. pores in GaAs do not seem to express the space–charge region width in an easily recognizable way.

The diameters of some pores (again, most prominently the GaAs pores), does not seem to express any of the length scales mentioned so far; this is especially true if the oscillations producing tetrahedra chains are considered.

In contrast to Si, parts of the pore geometry may not really express an intrinsic length scale, but the vagaries of nucleation. Repeated branching because too few pores were nucleated may not be finished by the time the experiment is stopped and the pore structure then does not express a stable equilibrium situation. The distance between the pores then is not a significant length, while the diameter still is.

7.2. Pore-Formation Modeling and Self-Organization

It is evident that any pore formation modeling must explain the self-organization features observed. Generally speaking, the physical effects providing synchronization of local oscillations are more difficult to understand than the possible effects leading to local oscillations. While the chemistry of any given system certainly plays a major role in determining what is going to happen in an anodic etching experiment and provides for the basic differences between different materials, there must also be some general phenomena behind the general behavior, and here we will only comment on this part of formation models.

In the context of voltage oscillations, the basic assumption of an intrinsically oscillating current in any pore was already introduced and in view of the various experiments showing direct or indirect current–voltage oscillations in the context of semiconductor electrochemistry and pore formation, one might well except "pore-current oscillations" as one of the general phenomena occurring in most, if not all, pore etching experiments.

As a general reason for pore-current oscillations two (interrelated) reasons were proposed:

i) Current flow proceeds by "current bursts", i.e., charge transfers at the interface that are localized in time and space, and,

ii) Surface parts which are temporarily without current flow tend to passivate (after oxides have dissolved), i.e., reduce their density of interface states by covering the surface with

0935-9648/03/0302-0196 $ 17.50+.50/0

some passivating chemical species (H in the case of Si, Cl for GaAs,[89] but not many data are available for III–V materials). The passivation kinetics may be strongly orientation dependent (a known property for Si).

There might be several reasons for current bursts, e.g., ionic breakdown if oxides occurring at the very large field strength invariably encountered if an oxide becomes thinner during dissolution,[56] the local breakdown of passivated areas, or the unavoidable on/off situation for localized avalanche breakdown events. In any case, the system now has an intrinsic time constant (e.g., the average duration of a current burst, the average time between two current bursts), a definite prerequisite for any internal dynamics.

Surface passivation acts as a kind of negative feed-back mechanism for current burst nucleation. In well-passivated areas the Fermi energy of the semiconductor is not pinned to interface states, band-bending is possible and most of the applied potential drops in the space–charge region inside the semiconductor, thus reducing the potential at the interface and concomitantly the likelihood of nucleating a current burst. This essentially protects crystallographic planes which passivate fast on the expense of the slower ones and introduces at least part of the observed anisotropy in pore etching.

The internal dynamics are best expressed at low current densities since large external driving forces always tend to overwhelm internal dynamics. This condition corresponds to the formation of tetrahedra and octahedra chains which might be regarded as clearest expression of the internal system dynamics.

In a next step, interaction (in space and/or time) between individual current bursts may lead to correlation in time and/or space of the originally independent localized dissolution events; synchronization on a macroscopic scale may be observed.

More details can be found in the literature,[56] here it suffices to say that the ingredients of the general picture outlined here show some promise for explaining general features of pore etching and is unavoidable for some of the specific observations concerning large scale self-organization.

8. Conclusions

Pore formation in III–V semiconductors provides for fascinating cross-disciplinary research, combining semiconductor physics, nonlinear and quantum optics, electrochemistry, and stochastic physics/chemistry. The systems are intrinsically dynamic; this expresses itself at the deepest level by a strong tendency for current oscillations in a growing pore. A remarkable degree of self-organization and pattern formation may result from the system dynamics, and it is safe to say that many features are still awaiting discovery, not to mention explanation.

Pore formation in III–V semiconductors has greatly enlarged the data base about porous semiconductors and already has spawned new discoveries concerning pores in Si. While the results demonstrate that differences in basic chemistry and electrochemistry are certainly important, they also demonstrate that there is much common ground resulting from general semiconductor properties and self-organization features.

Even at the very early stage of investigation, porous layers in III–V material show a wealth of new properties, in particular huge nonlinear optical effects can be obtained. Applications of porous III–V semiconductors have to wait for more work in this general area of research, but are certainly feasible based on the findings obtained so far.

[1] L. T. Canham, *Appl. Phys. Lett.* **1990**, *57*, 1046.
[2] V. Lehmann, U. Gösele, *Appl. Phys. Lett.* **1991**, *58*, 856.
[3] T. Yonehara, presented at *Porous Semiconductors Science and Technology (PSST 2002)*, Tenerife, Spain, March, **2002**.
[4] R. B. Wehrspohn, J. Schilling, *MRS Bull.* **2002**, *26*, 623.
[5] O. Jessensky, F. Müller, U. Gösele, *Thin Solid Films* **1997**, *297*, 224.
[6] J. S. Shor, I. Grimberg, B.-Z. Weiss, A. D. Kurtz, *Appl. Phys. Lett.* **1993**, *62*, 2836.
[7] *Pits and Pores: Formation, Properties and Significance for Advanced Luminescent Materials* (Eds: P. Schmuki, D. J. Lockwood, H. S. Isaacs, A. Bsiesy), The Electrochemical Society, Montreal **1997**, pp. 97–9.
[8] B. D. Chase, D. B. Holt, *J. Electrochem. Soc.* **1972**, *119*, 314.
[9] M. M. Faktor, D. G. Fiddyment, M. R. Taylor, *J. Electrochem. Soc.* **1975**, *122*, 1566.
[10] H. Föll, J. Carstensen, S. Langa, M. Christophersen, I. M. Tiginyanu, PSST 2002, *Phys. Status Solidi. A* **2003**, in press.
[11] *Pits and Pores II: Formation, Properties and Significance for Advanced Materials* (Eds: P. Schmuki, D.J. Lockwood, Y. Ogata, and H.S. Isaacs), The Electrochemical Society, Phoenix, AR **2001**.
[12] S. Langa, M. Christophersen, J. Carstensen, I. M Tiginyanu, H. Föll, PSST 2002, *Phys. Status Solidi A* **2003**, in press.
[13] A. I. Belogorokhov, V. A. Karavanskii, A. N. Obraztsov, V. Yu. Timoshenco, *JETP Lett.* **1994**, *60*, 274.
[14] Anedda, A. Serpi, V. A. Karavanskii, I. M. Tiginyanu, V. M. Ichizli, *Appl. Phys. Lett.* **1995**, *67*, 3316.
[15] K. Kuriyama, K. Ushiyama, K. Ohbora, Y. Miyamoto, S. Takeda, *Phys. Rev. B* **1998**, *58*, 1103.
[16] B. H. Erne, D. Vanmaekelbergh, J. J. Kelly, *J. Electrochem. Soc.* **1996**, *143*, 305.
[17] F. Iranzo Marin, M. A. Hamstra, D. Vanmaekelbergh, *J. Electrochem. Soc.* **1996**, *3*, 1137.
[18] F. J. P. Schuurmans, D. Vanmaekelbergh, J. van de Lagemaat, A. Lagendijk, *Science* **1999**, *284*, 141.
[19] F. J. P. Schuurmans, M. Magens, D. Vanmaekelbergh, A. Lagendijk, *Phys. Rev. Lett.* **1999**, *83*, 2183.
[20] J. Gomez Rivas, A. Lagendijk, R. W. Tjerkstra, D. Vanmaekelbergh, J. J. Kelly, *Appl. Phys. Lett.* **2002**, *80*, 4498.
[21] M. A. Stevens-Kalceff, I. M. Tiginyanu, S. Langa, H. Föll, *J. Appl. Phys.* **2001**, *89*, 2560.
[22] I. M. Tiginyanu, I. V. Kravetsky, G. Marowsky, H. L. Hartnagel, *Phys. Status Solidi A* **1999**, *175*, R5.
[23] E. Kikuno, M. Amiotti, T. Takizawa, S. Arai, *Jpn. J. Appl. Phys.* **1995**, *34*, 177.
[24] I. M. Tiginyanu, G. Irmer, J. Monecke, H. L. Hartnagel, *Phys. Rev. B* **1997**, *55*, 6739.
[25] I. M. Tiginyanu, V. V. Ursaki, Y. S. Raptis, V. Stergiou, E. Anastassakis, H. L. Hartnagel, A. Vogt, B. Prevot, C. Schwab, *Phys. Status Solidi B* **1999**, *211*, 281.
[26] A. Liu, C. Duan, *Phys. E* **2001**, *9*, 723.
[27] M. Ohmukai, Y. Tsutumi, *Thin Solid Films* **1997**, *302*, 51.
[28] A. Liu, C. Duan, *Appl. Phys. Lett.* **2001**, *78*, 43.
[29] H. Fujikura, A. Liu, A. Hamamatsu, T. Sato, H. Hasegawa, *Jpn. J. Appl. Phys.* **2000**, *39*, 4616.
[30] A. Hamamatsu, C. Kaneshiro, H. Fujikura, H. Hasegawa, *J. Electroanal. Chem.* **1999**, *473*, 223.
[31] W. Bludau, *Halbleiter-Optoelektronik, Die physikalischen Grundlagen der LED's, Diodenlaser und pn-Photodioden*, Hanser Verlag, München-Wien **1995**.
[32] I. M. Tiginyanu, I. V. Kravetsky, J. Monecke, W. Cordts, G. Marowsky, H. L. Hartnagel. *Appl. Phys. Lett.* **2000**, *77*, 2415.

  0935-9648/03/0302-0197 $ 17.50+.50/0

[33] E. K. Propst, P. A. Kohl, *J. Electrochem. Soc.* **1994**, *141*, 1006.
[34] M. Christophersen, J. Carstensen, A. Feuerhake, H. Föll, *Mat. Sci. Eng. B* **2000**, *69–70*, 194.
[35] P. Schmuki, J. Fraser, C. M. Vitus, M. J. Graham, H. S. Isaacs, *J. Electrochem. Soc.* **1996**, *143*, 3316.
[36] H. Gerischer , I. Wallem-Mattes, *Z. Phys. Chem.* **1969**, *64*, 187.
[37] S. R. Morrison, *J. Appl. Phys.* **1982**, *52*, 1233.
[38] X. G. Zhang, *J. Electrochem. Soc.* **1991**, *138*, 3750.
[39] R. Memming, in *Electroanalytical Chemistry. A Series of Advances*, Vol. 11. (Ed: A. J. Bard), Marcel Dekker, New York **1979**, Ch. 1.
[40] B. P. Minks, D. Vanmaekelbergh, J. J. Kelly, *J. Electroanal. Chem.* **1989**, *273*, 133.
[41] Kaneshiro, T. Sato, H. Hasegawa, *Jpn. J. Appl. Phys.* **1999**, *38*, 1147.
[42] P. H. L. Notten, J. E. A. M. van den Meerakker, J. J. Kelly, *Etching of III–V semiconductors: An electrochemical approach*, Elsevier, Oxford **1991**.
[43] V. Lehmann, *Electrochemistry of Silicon*, Wiley-VCH, Weinheim **2002**.
[44] P. Schmuki, L. E. Erikson, D. J. Lockwood, B. F. Mason, J. W. Fraser, G. Champion, H. J. Labbe, *J. Electrochem. Soc.* **1999**, *146*, 735.
[45] P. Schmuki, L. E. Erickson, D. J. Lockwood, J. W. Fraser, G. Champion, H. J. Labbe, *Appl. Phys. Lett.* **1998**, *72*, 1039.
[46] P. Schmuki, L. Santinacci, T. Djenizian, D. J. Lockwood, *Phys. Status Solidi A* **2000**, *182*, 51.
[47] R. W. Tjerkstra, J. Gomez-Rivas, D. Vanmaekelbergh, J. J. Kelly, *Electrochem. Solid-State Lett.* **2002**, *5*, G32.
[48] P. Müller, IUPAC Manual of Symbols and Technology, *Pure Appl. Chem.* **1972**, *31*, 578, Appendix 2, Part 2.
[49] I. M. Tiginyanu, I. V. Kravetsky, S. Langa, G. Marowsky, J. Monecke, H. Föll, PSST 2002 *Phys. Status Solidi A* **2003**, in press.
[50] S. Langa, I. M. Tiginyanu, J. Carstensen, M. Christophersen, H. Föll, *Electrochem. Solid-State Lett.* **2000**, *3*, 514
[51] C. Levy-Clement, A. Lagoubi, M. Tomkiewitch. *J. Electrochem. Soc*. **1994**, *141*, 958.
[52] T. Osaka, K. Ogasawara, and S. Nakahara, *J. Electrochem. Soc*. **1997**, *144*, 3226.
[53] Y. Morishita, S. Kowai, J. Sunagawa, T. Suzuki, *Electrochem. Solid-State Lett.* **2001**, *4*, G4.
[54] J. C. Tranchart, L. Hollan, R. Memming, *J. Electrochem. Soc.* **1978**, *125*, 1185.
[55] V. Lehmann, R. Stengel, A. Luigart, *Mater. Sci. Eng. B* **2000**, *69–70*, 11.
[56] J. Carstensen, M. Christophersen, H. Föll, *Mater. Sci. Eng. B* **2000**, *69–70*, 23.
[57] V. Lehmann, *J. Electrochem. Soc.* **1996**, *143*, 1313.
[58] J. Carstensen, R. Prange, G. S. Popkirov, H. Föll, *Appl. Phys. A* **1998**, *67*, 459.
[59] F. M. Ross, G. Oskam, P. C. Searson, J. M. Macaulay, J. A. Liddle, *Philos. Mag. A* **1997**, *75*, 525.
[60] M. Hao, H. Uchida, T. Soga, T. Jombo, M. Umeno, *J. Cryst. Growth* **1997**, *179*, 661.
[61] S. Langa, J. Carstensen, M. Christophersen, H. Föll, I. M. Tiginyanu, *Appl. Phys. Lett.* **2001**, *78*, 1074.
[62] P. Allongue, C. Henry de Villeneuve, L. Pinsard, M. C. Bernard, *Appl. Phys. Lett.* **1995**, *67*, 7.
[63] V. Lehmann, *J. Electrochem Soc.* **1993**, *140*, 2836.
[64] I. M. Tiginyanu, C. Schwab, J.-J. Grob, B. Prevot, H. L. Hartnagel, A. Vogt, G. Irmer, J. Monecke, *Appl. Phys. Lett.* **1997**, *71*, 3829.
[65] M. M. Carrabba, N. M. Nguyen, R. D. Rauh, *J. Electrochem. Soc.* **1987**, *134*, 1855.
[66] H. Föll, S. Langa, J. Carstensen, M. Christophersen, presented at *MRS Spring Meeting*, San Francisco, USA, April **2002**.
[67] T. Takizawa, S. Arai, M. Nakahara, *Jpn. J. Appl. Phys.* **1994**, *54*, L643.
[68] S. Langa, J. Carstensen, I. M. Tiginyanu, M. Christophersen, H. Föll, *Electrochem. Solid-State Lett.* **2001**, *4*, G50.
[69] E. Harvey, D. N. Buckley, S. N. G. Chub, *Electrochem. Solid-State Lett.* **2002**, *5*, G22.
[70] M. Christophersen, S. Langa, J. Carstensen, I. M. Tiginyanu, H. Föll, PSST 2002 *Phys. Status Solidi A* **2003**, in press.
[71] M. Christophersen, K. Voigt, presented at the *International Workshop on Porous III–V materials*, Kiel, Germany, October **2001**.
[72] J. E. A. N. van den Meerakker, R. J. G. Elfrink, W. M. Weeda, *Phys. Status Solidi A* **2002**, in press.
[73] I. M. Tiginyanu, V. V. Ursaki, V. A. Karavanskii, V. N. Sokolov, Y. S. Raptis, E. Anastassakis, *Solid State Commun.* **1996**, *97*, 675.
[74] W. P. Gomes, H. H. Goossens, in *Advances in Electrochemical Science and Engineering* (Eds: H. Gerischer, C.W. Tobias) VCH, Weinheim, **1994**.
[75] T. Takebe, T. Yamamoto, M. Fujii, K. Kobayashi, *J. Electrochem. Soc.* **1993**, *140*, 1169.
[76] It should be noted that in the literature a second definition can be found. In this case, the ⟨111⟩ directions point from B to A planes along the longest (not shortest) distance between these planes. The authors think that the first definition is more appropriate to describe the dissolution process.
[77] S. Langa, J. Carstensen, M. Christophersen, H. Föll, I. M. Tiginyanu, in *Selfordering in Porous III–V Compounds, in Ordered Pore Systems* (Ed: R. B. Wehrspohn) Springer, Berlin **2003**.
[78] C. Jäger, B. Finkenberger, W. Jäger, M. Christophersen, J. Carstensen, H. Föll, *Mater. Sci. Eng. B* **2000**, *69–70*, 199.
[79] S. Langa, J. Carstensen, I. M. Tiginyanu, M. Christophersen, H. Föll, *Electrochem. Solid-State Lett.* **2002**, *5*, C14.
[80] R. Arens-Fischer, M. Krüger, M. Thönissen, V. Ganse, D. Hunkel, M. Marso, L. Lüth, *J. Porous Mater.* **2000**, *7*, 223.
[81] E. K. Squire, P. A. Show, P. S. J. Russel, L. T. Canham, A. J. Simons, C. L. Reeves, D. J. Wallis, *J. Porous Mater.* **2000**, *7*, 209.
[82] H. Masuda, K. Yada, A. Osaka, *Jpn. J. Appl. Phys.* **1998**, *37*, L1340.
[83] A.-P. Li, F. Müller, U. Gösele, *Electrochem. Solid-State Lett.* **2000**, *3*, 131.
[84] J. Grzanna, H. Jungblut, H. J. Lewerenz, *J. Electroanal. Chem*. **2000**, *486*, 181.
[85] H. Föll, J. Carstensen, M. Christophersen, G. Hasse, presented at *Electrochemical Society Fall Meeting*, Phoenix, AZ, September **2000**.
[86] J. Schilling, F. Müller, S. Matthias, R. B. Wehrspohn, U. Gösele, K. Busch, *Appl. Phys. Lett.* **2001**, *78*, 1180.
[87] J.-N. Chazalviel, R. B. Wehrspohn, F. Ozanam, *Mater. Sci. Eng. B* **2000**, *69–70*, 1.
[88] H. Föll, J. Carstensen, M. Christophersen, G. Hasse, *Phys. Status Solidi A* **2000**, *182*, 7.
[89] Z. H. Lu, T. Tyliszczak, A. P. Hitschcock, *Phys. Rev. B* **1998**, *58*, 13 820.

  0935-9648/03/0302-0198 $ 17.50+.50/0